Recovery of Monoclinic phase of VO_2 Nanoparticles from Oxidized Samples: Assessment of Reusability and Optimization of Re-annealing Conditions

ABSTRACT

Vanadium dioxide (VO_2) nanoparticles in the monoclinic (M) phase exhibit a reversible metal–insulator transition (MIT) at ~68 °C, underpinning thermochromic applications such as smart windows and thermal sensors. However, prolonged atmospheric exposure causes progressive surface oxidation that converts V^{4+} to V^{5+}, leading to phase degradation and loss of thermochromic function. This study demonstrates that oxidized VO_2 nanopowders can be fully recovered by thermal re-annealing in an inert argon atmosphere. Starting from VO_2(M) nanoparticles synthesized via a hydrothermal route, controlled oxidation under ambient conditions produced a degraded sample rich in V_2O_5. Systematic re-annealing at 450-600 °C for 2-3 h identified 500 °C for 2 h as the optimal recovery condition. XRD, Raman spectroscopy, and UV-Vis-NIR transmittance measurements confirm complete phase restoration and recovery of thermochromic switching performance equivalent to the as-synthesized material, establishing a practical strategy for reusing degraded VO_2 nanopowder stocks.

Keywords: vanadium dioxide*, smart window, transition material, thermochromic recovery.*

1. INTRODUCTION

Vanadium dioxide (VO_2) is a polymorphic transition-metal oxide capable of adopting several crystal structures-monoclinic (M), VO_2(A), VO_2(B), and VO_2(D) - despite sharing the same chemical composition. [1]-[3] The differences among these polymorphs arise from distinct VO_6 octahedral arrangements within the crystal lattice, giving each phase unique structural and electronic properties (Figure. 1).

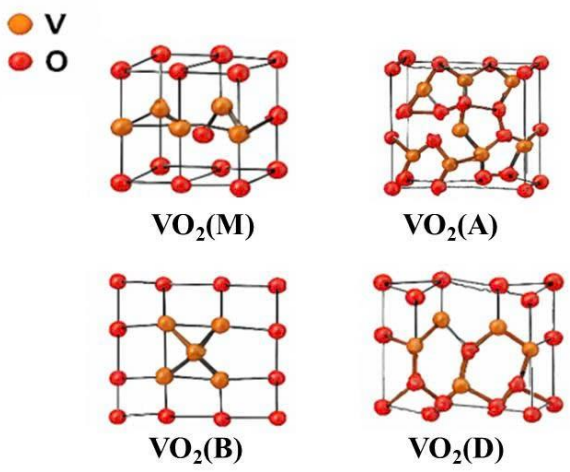

Figure 1. Crystal lattice structures of the four VO_2 polymorphs: VO_2(M), VO_2(A), VO_2(B), and VO_2(D). Orange: V atoms; red: O atoms.

Among these, monoclinic VO_2(M) is thermodynamically stable at room temperature and is of exceptional importance owing to its reversible semiconductor–metal phase transition near 340 K (~68 °C), first reported by Morin. [4] In the monoclinic state, vanadium atoms form paired dimers along the c-axis, opening a band gap and yielding semiconducting behavior. Upon heating, dimerization disappears, the density of states near the Fermi level increases sharply, and metallic conductivity is recovered. [4][5] This structural reorganization also reverses the optical response: below the transition temperature, VO_2 transmits near-infrared (NIR) radiation; above it, the metallic phase strongly reflects NIR light. [6][7] This reversible electro-optical switching underpins thermochromic smart windows, thermal sensors, and optical limiters.

A variety of synthesis strategies have been developed for VO_2, including physical vapor deposition, magnetron sputtering, sol–gel, and hydrothermal methods. [8][9] Hydrothermal synthesis is particularly attractive because it permits direct control of crystal phase, particle size, and morphology through adjustment of temperature, pH, and redox atmosphere. [10][11] Typically, a V^{5+} precursor such as V_2O_5 is reduced to V^{4+} under hydrothermal conditions, yielding metastable VO_2(B) or VO_2(A) that is subsequently annealed to phase-pure VO_2(M) in an inert atmosphere. [10]-[12]

Despite extensive research, the storage stability of synthesized VO_2 nanopowders remains a practical challenge. Even in nominally sealed environments, prolonged ambient exposure causes gradual surface oxidation of V^{4+} to V^{5+}, forming V_2O_5-rich surface layers that broaden the MIT, reduce thermochromic contrast, and impair switching performance. [1][13] The nanoscale morphology of these

particles accelerates this degradation relative to bulk material owing to high surface-to-volume ratios. Recovery of degraded VO_2 nanopowders by thermal re-annealing in inert or reducing atmospheres has been proposed, [12][14] yet systematic optimization of re-annealing conditions for nanopowder specimens remains sparse in the literature.

In the present work, we synthesized VO_2(M) nanoparticles by a hydrothermal route, intentionally oxidized them under ambient conditions, and conducted systematic re-annealing in argon across temperatures of 450–600 °C and durations of 2–3 h. XRD, Raman spectroscopy, and UV-Vis-NIR transmittance measurements are used to track phase evolution and verify restoration of thermochromic function. Our results identify 500 °C_2 h as the optimal condition, demonstrating a straightforward, cost-effective protocol for reusing degraded VO_2 nanoparticle batches.

2. EXPERIMENTAL SECTION

2.1. Materials

Vanadium pentoxide (V_2O_5, ≥ 98%), concentrated sulfuric acid (H_2SO_4, 98%), hydrazine hydrate ($N_2H_4 \cdot H_2O$, 50–60 %), sodium hydroxide (NaOH, ≥ 95%), polyvinylpyrrolidone (PVP, MW = 40,000 g/mol), and absolute ethanol (99.6%) were used as received. Deionized (DI) water was used throughout.

2.2. Synthesis of VO_2(M) nanoparticles

VO_2(M) nanoparticles were prepared via a four-step hydrothermal procedure illustrated in Figure. 2.

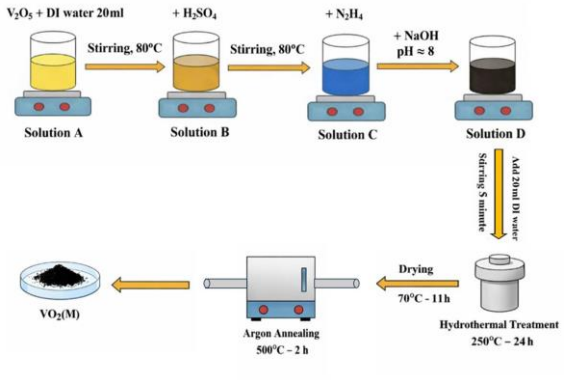

Figure 2. Schematic of the hydrothermal synthesis route for VO_2(M) nanoparticles, from V_2O_5 precursor dissolution to argon annealing.

Step 1: Precursor preparation: 0.9 g of V_2O_5 was dispersed in 20 mL DI water under stirring at 60 °C (Solution A, yellow suspension). Then 1.5 mL of H_2SO_4 was added dropwise at 80 °C to give a deep-yellow solution (Solution B).

Step 2: Reduction and pH adjustment: 0.5 mL of N_2H_4 was introduced dropwise, raising the temperature to 90-100 °C and yielding a blue solution (Solution C, pH ≈ 0.8-1). NaOH (2.3 g) was then added to adjust pH to ~8, producing a dark-brown suspension (Solution D). The color evolution is shown in Figure 3.

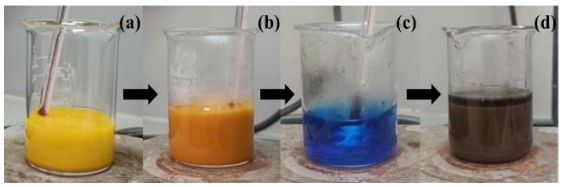

Figure 3. Optical photographs of the precursor at each synthesis step: (a) yellow V_2O_5 suspension; (b) deep-yellow Solution B; (c) blue Solution C after N_2H_4 reduction; (d) dark-brown Solution D after pH adjustment.

Step 3: Hydrothermal treatment: the precursor was transferred to a 25 mL Teflon-lined stainless-steel autoclave and heated at 250 °C for 24 h (5 °C min^{-1}).

Step 4: Post-treatment and annealing: the black precipitate was washed twice with DI water and once with ethanol, dried at 70 °C for 11 h, then annealed at 500 °C for 2 h in flowing Ar (10 °C min^{-1}) to obtain phase-pure VO_2(M).

2.3. Controlled oxidation

Synthesized VO_2(M) powders were stored in an open beaker under ambient laboratory conditions (~25 °C, relative humidity 60-70%) for a controlled period to simulate real-world aging. Color changes were recorded photographically; the fully oxidized sample was characterized by XRD, Raman, and UV-Vis-NIR spectroscopy.

2.4. Recovery by re-annealing

Oxidized powders were re-annealed in a tube furnace under continuous Ar flow. Stage 1 (temperature optimization): re-annealing at 450, 500, 550, and 600 °C for 2 h. Stage 2 (duration optimization): re-annealing at 500 °C for 2 h and 3 h. All heating ramps were 10 °C min^{-1}.

2.5. Characterization

Crystal structure was determined by X-ray diffraction (XRD, Cu Kα, λ = 0.15406 nm). Raman spectra were collected with a 532 nm laser excitation. Particle morphology was examined by scanning electron microscopy (SEM). Thermochromic performance was evaluated by UV-Vis-NIR transmittance spectroscopy (300-2000 nm) with a temperature-controlled stage during heating and cooling cycles between 30 and 100 °C. Integrated luminous transmittance (T_{lum}, 380-780 nm) and solar transmittance (T_{sol}, 250-

2600 nm) were calculated from the transmittance spectra.

3. RESULTS AND DISCUSSION

3.1. As-synthesized VO_2(M) nanoparticles

The hydrothermal synthesis and Ar annealing steps produced a jet-black powder (Figure. 4, right), in stark visual contrast to the yellow V_2O_5 precursor (Fig. 4, left). The color change reflects successful $V^{5+} \rightarrow V^{4+}$ reduction and VO_2(M) phase formation.

Photograph of yellow V_2O_5 powder | Photograph of black VO_2(M) powder

Figure 4. Optical photographs of the yellow V_2O_5 precursor powder (left) and the as-synthesized black VO_2(M) nanoparticle powder (right).

The UV-Vis-NIR transmittance spectra of original sample (Figure. 5) show a pronounced divergence between the 30 °C (semiconducting) and 100 °C (metallic) curves in the NIR region (800-2000 nm), confirming active thermochromic switching through the MIT at ~68 °C. [15] This large NIR transmittance contrast is the key functional signature of high-quality VO_2(M).

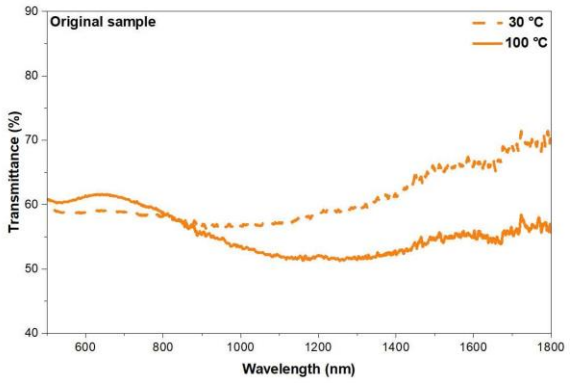

Figure 5. UV-Vis-NIR transmittance spectra of as-synthesized VO_2(M) film (Original sample) at 30 °C (dash line) and 100 °C (solid line), showing clear thermochromic NIR switching.

3.2. Oxidation behavior under ambient conditions

When VO_2(M) powder was stored in an open beaker under ambient air (Figure. 6), a progressive color transformation was observed over the course of days to weeks: black → bluish-black → moss green → dark moss green (Figure. 7). This sequence mirrors the gradual oxidation of V^{4+} to V^{5+} and accumulation of V_2O_5-like surface species.

Optical image of an empty beaker | Optical photograph of the beaker containing VO_2 sample after approximately one week

Figure 6. Storage experiment: empty reference beaker (left) and VO_2 powder sample after ~one week of ambient air exposure (right).

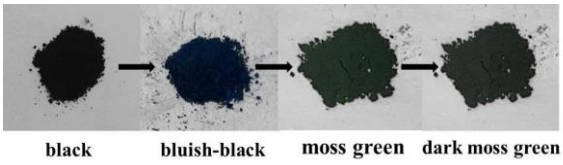

Figure 7. Time-dependent color evolution of VO_2 powder during ambient oxidation: black → bluish-black → moss green → dark moss green.

XRD analysis of the oxidized sample (Figure. 8) reveals emergence of V_2O_5 reflections alongside diminished VO_2(M) peaks, confirming phase transformation rather than mere surface contamination. [16] The original sample (orange) displays only sharp VO_2(M) reflections, while the oxidized sample (cyan) shows clear additional peaks at positions characteristic of V_2O_5 at 2 theta poisitions of 26.2°, 31°, 32.4°, 41°, 52° and 62°. Nevertheless, the persistence of lower-intensity peaks at 27.9°, 37°, 55°, 65° and 70° indicates a residual VO_2(M) component. Furthermore, the diffractogram suggests the secondary presence of the VO_2(B) phase as an impurity.

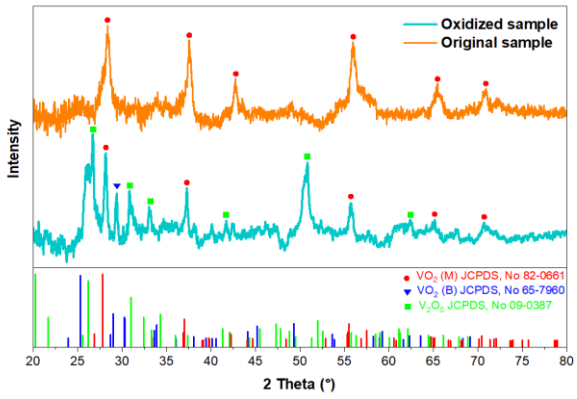

Figure 8. XRD patterns of the original VO_2(M) (orange) and oxidized sample (cyan) compared with reference stick patterns for VO_2(B) (blue), V_2O_5

(green) and VO_2(M) (red). Dashed lines mark key VO_2(M) peak positions.

The optical consequences are decisive: Figure. 9 shows UV-Vis-NIR spectra of the oxidized sample at 30 and 100 °C. The near-identical curves confirm complete abolition of thermochromic switching. [17] This finding is consistent with reports that even partial V^{5+} contamination can substantially suppress MIT sharpness, particularly in nanoparticle systems with high surface-to-volume ratios.

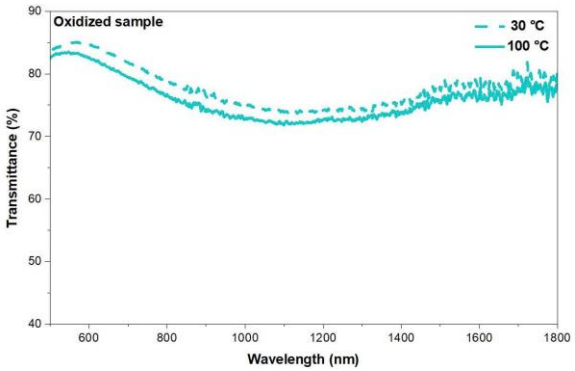

Figure 9. UV-Vis-NIR transmittance spectra of the oxidized sample at 30 °C (dash line) and 100 °C (solid line). Near-identical curves confirm complete suppression of the thermochromic MIT.

Raman spectroscopy further corroborates the phase loss (Figure. 10). The oxidized sample displays a featureless, monotonically rising background with no discernible VO_2(M) phonon modes, consistent with a V_2O_5-dominated surface that lacks the characteristic V-V dimerization modes of the monoclinic lattice.

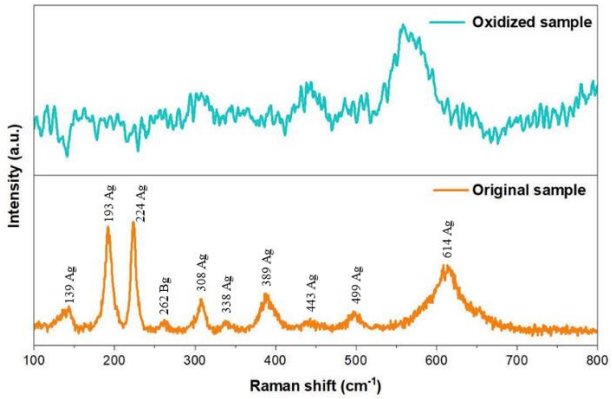

Figure 10. Raman spectrum of the oxidized VO_2 sample versus synthesized one. The featureless background and absence of VO_2(M) modes confirm complete disruption of the monoclinic lattice.

3.3. Recovery of VO_2(M) by thermal re-annealing

Re-annealing in Ar provides a mild reducing environment that drives the thermodynamically favorable conversion $V_2O_5 \rightarrow VO_2$ without introducing unwanted dopants or secondary reactions. The phase evolution was tracked visually (Figure. 11) and by XRD (Figure. 12).

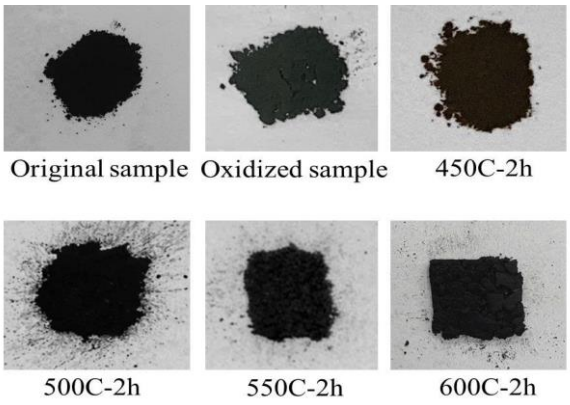

Figure 11. Optical photographs comparing original VO_2(M), oxidized sample, and re-annealed samples at 450, 500, 550, and 600 °C (2 h each). The 500-600 °C samples recover the characteristic black color.

In Figure. 12, re-annealing at 450 °C (black trace) yields broad, poorly resolved peaks with poor agreement to the VO_2(M) reference - indicating incomplete reduction. At 500 °C (pink trace), a clean pattern matching the VO_2(M) reference (red sticks) is obtained with no V_2O_5 or VO_2(B) impurities. At 550 °C and 600 °C, additional peaks inconsistent with VO_2(M) appear, attributable to minor VO_2(B) or over-reduced secondary phases. [18]

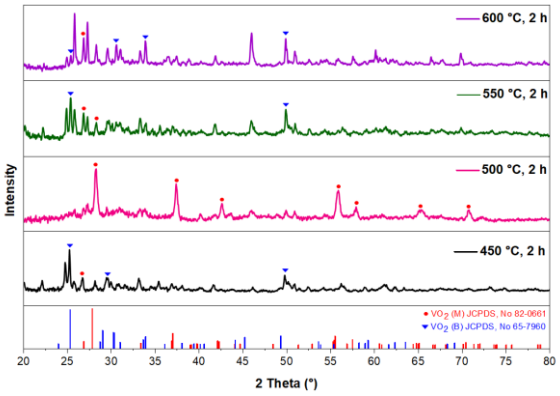

Figure 12. XRD patterns of samples re-annealed at 450 °C (black), 500 °C (pink), 550 °C (dark green), and 600 °C (purple), with VO_2(B) (blue) and VO_2(M) (red) reference patterns.

Raman spectroscopy of the 500 °C_2 h sample, Figure. 13 confirms the reappearance of sharp VO_2(M) phonon modes at ~224 and ~614 cm^{-1}, with additional features at ~139, ~193, ~262, ~308, ~338, ~389, ~443, and ~499 cm^{-1}- all characteristic of the monoclinic lattice and V-V dimerization. No V_2O_5 Raman bands are visible, providing unambiguous spectroscopic confirmation of complete phase recovery.

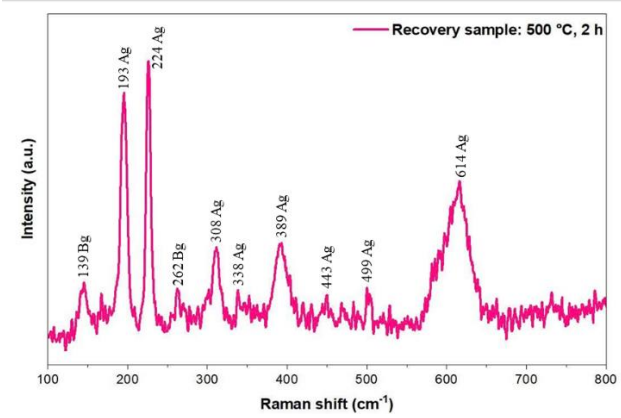

Figure 13. Raman spectrum of recovered VO_2(M) (500 °C_2 h). Characteristic VO_2(M) modes at ~220 and ~610 cm^{-1} are clearly restored.

3.4. Optimization of Re-annealing Duration

Comparing re-annealing at 500 °C for 2 h versus 3 h reveals a critical narrow processing window (Figure. 14). The 2 h sample (left, pink) yields a phase-pure VO_2(M) XRD pattern with no extraneous reflections. Extending the duration to 3 h (right, purple) introduces VO_2(B) peaks (highlighted by dashed lines), indicating the onset of over-reduction or phase instability under prolonged thermal treatment. Therefore, 2 h is the optimal duration-sufficient for complete reduction yet short enough to avoid unwanted phase evolution.

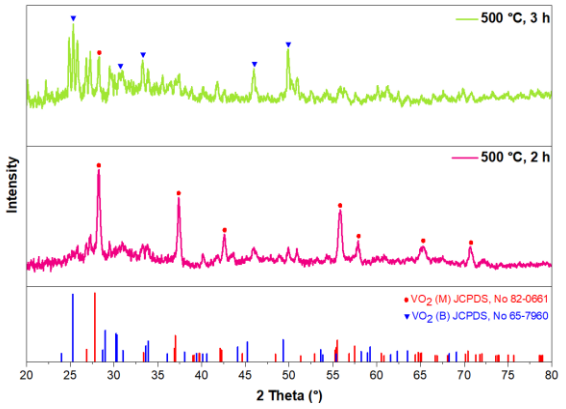

Figure 14. XRD comparison of re-annealing at 500 °C for 2 h (pink, left) and 3 h (lime green, right). The 3 h sample shows VO_2(B) impurity peaks (dashed lines), confirming 2 h as optimal.

3.5. Verification of thermochromic performance restoration

Figure. 15 presents UV-Vis-NIR data for the optimally recovered sample (500 °C_2 h). The spectra shows a pronounced divergence between the 30 and 100 °C curves in the NIR region, fully restoring the thermochromic switching behavior of the original material. The recovered NIR contrast and switching temperature (~68 °C) are quantitatively equivalent to those of the original as-synthesized sample.

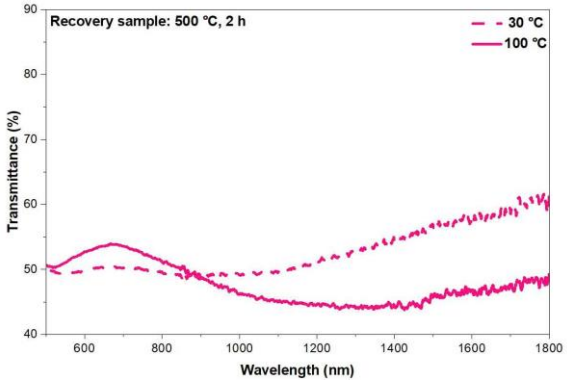

Figure 15. Characterization of recovered VO_2(M) (500 °C_2 h): UV-Vis-NIR transmittance spectra at 30 °C (dash line) and 100 °C (solid line) confirming full thermochromic recovery.

The complete restoration of the MIT - a property exquisitely sensitive to stoichiometry, lattice order, and surface chemistry - confirms that re-annealing at the optimal condition drives thorough phase recovery, extending from the nanoparticle surface into the bulk. This result is consistent with previous reports on thin-film VO_2 systems where post-synthesis reduction treatments restored MIT sharpness and thermochromic contrast. [2][14][19][20] The practical significance is considerable: VO_2 nanoparticle synthesis requires multi-step procedures, specialized equipment, and expensive precursors. Rejuvenating oxidized stocks via a single 2-hour Ar annealing step - identical to the original synthesis annealing - eliminates the need to discard and resynthesize degraded material, reducing cost, waste, and synthesis time.

4. CONCLUSION

This study has systematically demonstrated the feasibility of recovering phase-pure monoclinic VO_2(M) nanoparticles from ambient-oxidized nanopowders through thermal re-annealing in argon. Progressive atmospheric oxidation converted V^{4+} to V^{5+}, yielding V_2O_5 - rich phases that completely suppressed the MIT, as evidenced by XRD, Raman spectroscopy, and UV-Vis-NIR transmittance. Systematic re-annealing experiments across 450–600 °C and 2–3 h identified 500 °C_2 h in Ar as the optimal recovery condition. Under these conditions, XRD and Raman spectroscopy confirmed complete VO_2(M) phase restoration, and UV-Vis-NIR measurements verified quantitative recovery of thermochromic performance equivalent to the original as-synthesized nanoparticles. These results provide a practical, scalable protocol for

extending the operational lifetime of VO_2 nanopowder batches, with direct implications for reducing material waste and cost in thermochromic device fabrication.

ACKNOWLEDGMENTS

The authors gratefully acknowledge the VLIR-UOS, Belgium, and Quy Nhon University for supporting this work under the project codes VN2022IUC044A101 and S2025.1152.102

REFERENCES

[1] F. J. Morin, "Oxides which show a metal-to-insulator transition at the Néel temperature," Physical Review Letters, vol. 3, no. 1, pp. 34–36, 1959.

[2] J. Liu, Q. Li, T. Wang, D. Yu, and Y. Li, "Thermochromic VO_2 thin film prepared by post annealing treatment of V_2O_5 thin film," Advanced Materials Research, vols. 79–82, pp. 747–750, 2009.

[3] *S*. Liang, J. Shi, H. Zheng, B. Liu, Q. Liu, and C. Li, "A facile pathway to prepare VO_2 and V_2O_3 powders via carbothermal reduction," Journal of Solid State Chemistry, vol. 265, pp. 299–305, 2018.

[4] D. K. Manousou, *E*. Gagaoudakis, G. Michail, V. Binas, G. Kiriakidis, V. Diakonov, and M. Kompitsas, "VO_2 thin films fabricated by reduction of thermally evaporated V_2O_5 under N_2 flow," Materials Letters, vol. 299, p. 130086, 2021.

[5] *Z*. Yang, C. Ko, and *S*. Ramanathan, "Oxide electronics utilizing ultrafast metal-insulator transitions," Annual Review of Materials Research, vol. 41, pp. 337–367, 2011.

[6] C. G. Granqvist, "Electrochromics for smart windows: oxide-based thin films and devices," Thin Solid Films, vol. 564, pp. 1–38, 2014.

[7] M. M. Qazilbash et al., "Mott transition in VO_2 revealed by infrared spectroscopy and nano-imaging," Science, vol. 318, no. 5857, pp. 1750–1753, 2007.

[8] A. Kumar, A. Kumar, A. Kandasami, and V. *R*. Singh, "A comprehensive review on synthesis, phase transition, and applications of VO_2," Journal of Superconductivity and Novel Magnetism, vol. 37, no. 3, pp. 475–498, 2024.

[9] J. Chen, X. Tian, L. Ye, P. Lu, Q. Luo, J. Yan, and D. Zhang, "High-performance VO_2 thin film prepared via room-temperature-deposition and air-annealing treatment," Journal of Electronic Materials, vol. 54, no. 9, pp. 7935–7941, 2025.

[10] W. Burkhardt et al., "Tungsten and fluorine co-doping of VO_2 films," Thin Solid Films, vol. 402, no. 1–2, pp. 228–234, 2002.

[11] Y. Gao, H. Luo, *Z*. Zhang, L. Kang, *Z*. Chen, J. Du, M. Kanehira, and C. Cao, "Nanoceramic VO_2 thermochromic smart glass: a review on progress in solution processing," Nano Energy, vol. 1, no. 2, pp. 221–246, 2012.

[12] M. Soltani, M. Chaker, *E*. Haddad, *R*. V. Kruzelecky, and J. Margot, "Effects of Ti-W codoping on the optical and electrical switching of vanadium dioxide thin films grown by a reactive pulsed laser deposition," Applied Physics Letters, vol. 85, no. 11, pp. 1958–1960, 2004.

[13] Y. Gao et al., "Enhanced chemical stability of VO_2 nanoparticles by the formation of SiO_2/VO_2 core/shell structures and the application to transparent and flexible VO_2-based composite foils with excellent thermochromic properties for solar heat control," Energy & Environmental Science, vol. 5, pp. 6104–6110, 2012.

[14] K. Araki, K. Bando, K. Takahashi, H. Watanabe, T. Yokoyama, and M. Fujii, "Maximizing infrared transmission contrast of VO_2 thin films by thermal reduction processing," arXiv, 2503.09241, 2025.

[15] *Z*. Liang et al., "Long-term stability and efficiency of VO_2 nanostructure-based thermochromic smart windows," ACS Applied Nano Materials, vol. 7, no. 18, pp. 21683–21691, 2024.

[16] Y. Yang et al., "Suppression of photoinduced surface oxidation of vanadium dioxide nanostructures by blocking oxygen adsorption," ACS Omega, vol. 4, no. 18, pp. 17735–17740, 2019.

[17] J. Cao et al., "Strain engineering and one-dimensional organization of metal-insulator domains in single-crystal vanadium dioxide beams," Nature Nanotechnology, vol. 4, no. 11, pp. 732–737, 2009.

[18] L. Kang, Y. Gao, H. Luo, *Z*. Chen, J. Du, and *Z*. Zhang, "Nanoporous thermochromic VO_2 films with low optical constants, enhanced luminous transmittance and thermochromic properties," ACS Applied Materials & Interfaces, vol. 3, no. 2, pp. 135–138, 2011.

[19] M. Kumar, *S*. Rani, J. P. Singh, K. H. Chae, Y. Kim, J. Park, and H. H. Lee, "Structural phase control and thermochromic modulation of VO_2 thin films by post thermal annealing," Applied Surface Science, vol. 529, p. 147093, 2020.

[20] *S*. Wang, M. Liu, L. Kong, Y. Long, X. Jiang, and A. Yu, "Recent progress in VO_2 smart coatings: strategies to improve the thermochromic properties," Progress in Materials Science, vol. 81, pp. 1–54, 2016.

Phục hồi pha tinh thể đơn tà của hạt nano vo_2 từ mẫu bị oxy hóa: đánh giá khả năng tái sử dụng và tối ưu điều kiện nung phục hồi

TÓM TẮT

Các hạt nano vanadium dioxide (VO_2) pha đơn tà (M) có khả năng chuyển đổi pha giữa kim loại - bán dẫn (MIT) thuận nghịch tại ~68 °C đã mở ra các ứng dụng nhiệt sắc như cửa sổ thông minh và cảm biến nhiệt. Tuy nhiên, việc phơi nhiễm trong môi trường khí quyển gây ra hiện tượng oxy hóa bề mặt, chuyển đổi V^{4+} thành V^{5+}, dẫn đến suy giảm chất lượng pha tinh thể hoặc thay đổi thành phần pha làm mất chức năng nhiệt sắc. Trong nghiên cứu này, các hạt nano VO_2 bị oxy hóa cho thấy khả năng được phục hồi hoàn toàn bằng cách nung lại trong môi trường khí trơ. Từ các hạt nano VO_2(M) được tổng hợp bằng phương pháp thủy nhiệt, quá trình oxy hóa có kiểm soát được thực hiện trong điều kiện môi trường tạo ra mẫu bị chất lượng tinh thể bị suy giảm và chứa thành phần V_2O_5. Để khảo sát khả năng hồi phục pha tinh thể VO_2(M), quá trình nung lại được khảo sát hệ thống từ 450-600 °C trong 2-3 giờ, kết quả cho thấy nung ở điều kiện tại nhiệt độ 500 °C trong 2 giờ là điều kiện phục hồi tối ưu. Phép phân tích XRD, phổ Raman và đo phổ truyền qua UV- Vis-NIR cho thấy VO_2(M) khôi phục hoàn toàn pha và hiệu suất nhiệt sắc tương đương với vật liệu ban đầu.

Từ khóa: vanadium dioxide, *cửa sổ thông minh, vật liệu chuyển pha, hồi phục tính chất nhiệt sắc*